MATERIALS SCIENCE

Motion tracking of 80-nm-size skyrmions upon directional current injections

X. Z. Yu[1]*, D. Morikawa[1†], K. Nakajima[1], K. Shibata[1‡], N. Kanazawa[2], T. Arima[1,3], N. Nagaosa[1,2], Y. Tokura[1,2,4]

Nanometer-scale skyrmions are prospective candidates for information bits in low–power consumption devices owing to their topological nature and controllability with low current density. Studies on skyrmion dynamics in different classes of materials have exploited the topological Hall effect and current-driven fast motion of skyrmionic bubbles. However, the small current track motion of a single skyrmion and few-skyrmion aggregates remains elusive. Here, we report the tracking of creation and extinction and motion of 80-nm-size skyrmions upon directional one–current pulse excitations at low current density of the order of 10^9 A m^{-2} in designed devices with the notched hole. The Hall motion of a single skyrmion and the torque motions of few-skyrmion aggregates have been directly revealed. The results exemplify low–current density controls of skyrmions, which will pave the way for the application of skyrmions.

INTRODUCTION

The idea of racetrack-type memory based on the current-driven motion of the ferromagnetic (FM) domain wall (*1*) has a high impact on the spintronics field owing to its potential enabling the energy-efficient current control of magnetization for information processing. In general, moving the FM domain wall in terms of the spin transfer torque, thereby reversing the domain orientation, requires a high critical current density (J_C; typically 10^{12} A m^{-2}), which induces significant resistive heating in the device. To overcome this problem, a small J_C is required for drives of magnetic information carriers. Among many types of magnetic-information carriers, the skyrmion—a particle-like topological spin texture—has attracted enormous attention because of its nanometer-scale size, topological stability, and drivability with ultralow current density (e.g., 10^6 A m^{-2}) (*2*–*15*). Thus, the skyrmion is a promising candidate for future application to energy-efficient electronic devices. In the context of current-driven racetrack-type skyrmion memory, the isolated skyrmion, which can be manipulated in a metastable state (*9*, *16*–*19*), is of more importance than the skyrmion crystal (SkX) that is thermodynamically stabilized in chiral-/polar-lattice magnets with the intrinsic Dzyaloshinskii-Moriya interaction (DMI) (*2*, *3*, *6*). Thus, the interfaces between the heavy-metal layer and the ultrathin FM layer hosting isolated skyrmions caused by the interfacial DMI have been investigated extensively (*10*–*14*). However, compared with the small current density J_C for controls of SkX in chiral-lattice magnets with intrinsic DMI (*3*, *4*, *20*–*22*), driving of interfacial skyrmions requires higher J_C (~10^{12} A m^{-2}) to overcome the random pinning potential in the real material interfaces, which strongly depends on the film quality (*10*–*14*, *23*–*26*).

A key technology for the low-J_C manipulation of a single skyrmion is sought for, such as efficient and reliable control of generation and driving individual skyrmions in the chiral-lattice system. For this end, first, a successful skyrmion nucleation with low current density in the device must be achieved; second, the individual skyrmions must be isolated from the SkX; last, it is necessary to control, i.e., to drive and to erase, skyrmions.

Here, we introduce a device composed of a thin plate of FeGe (*27*) with the helimagnetic transition temperature of 278 K, which has a square notch hole so as to generate localized spin current around the notch corner (Fig. 1A, see also Methods in the Supplementary Materials for details). First, we demonstrate the generation and extinction of the metastable SkX composed of 80-nm-size skyrmions in terms of unidirectional current injections in the plus and minus directions, respectively. The unidirectional current effect on the skyrmion dynamics as demonstrated in the following could never appear in the device without such a notch, indicating that the local current distribution together with the modulated configuration of magnetic moments around the notch is crucial for this effect. After realizing the current-induced generation of the skyrmions in various forms such as regular lattice (SkX), single particle, and also a few-skrymion aggregate, which was observed as a metastable state formerly with tuning the external field in thin plates of FeGe (*17*) and Cu_2OSeO_3 (*28*), their current-induced motions are tracked by Lorentz transmission electron microscopy (TEM) to investigate the temporal dynamics.

RESULTS

First, we show the creation and extinction of skyrmions by current pulse excitations on the FeGe-based notched device (Fig. 1A and fig. S1). Figure 1B presents the phase diagram based on the sequential Lorentz TEM observations with varying the normal magnetic field (B) at several temperatures (Ts). A thermodynamic equilibrium SkX phase appears only in a small T-B pocket region near T_C and agrees well with our previous work (*17*), whereas nontopological spin textures, such as helical (H), conical (C), and field-aligned FM structures, are stabilized to dominate the T-B phase diagram, being somewhat different from the case observed in the same-material thin plate but with different sample geometry (*29*). A metastable SkX (Fig. 1D) has been successfully created by only one current pulse injection (8 mA, 100-ms duration) from a helical structure (Fig. 1C) in the "plus"

[1]RIKEN Center for Emergent Matter Science (CEMS), Wako 351-0198, Japan. [2]Department of Applied Physics, University of Tokyo, Tokyo 113-8656, Japan. [3]Department of Advanced Materials Science, University of Tokyo, Kashiwa 277-8561, Japan. [4]Tokyo College, University of Tokyo, Tokyo 113-8656, Japan.
*Corresponding author. Email: yu_x@riken.jp
†Present address: Institute of Multidisciplinary Research for Advanced Materials, Tohoku University, Sendai, Miyagi, Japan.
‡Present address: Institute of Industrial Science, University of Tokyo, Tokyo, Japan.

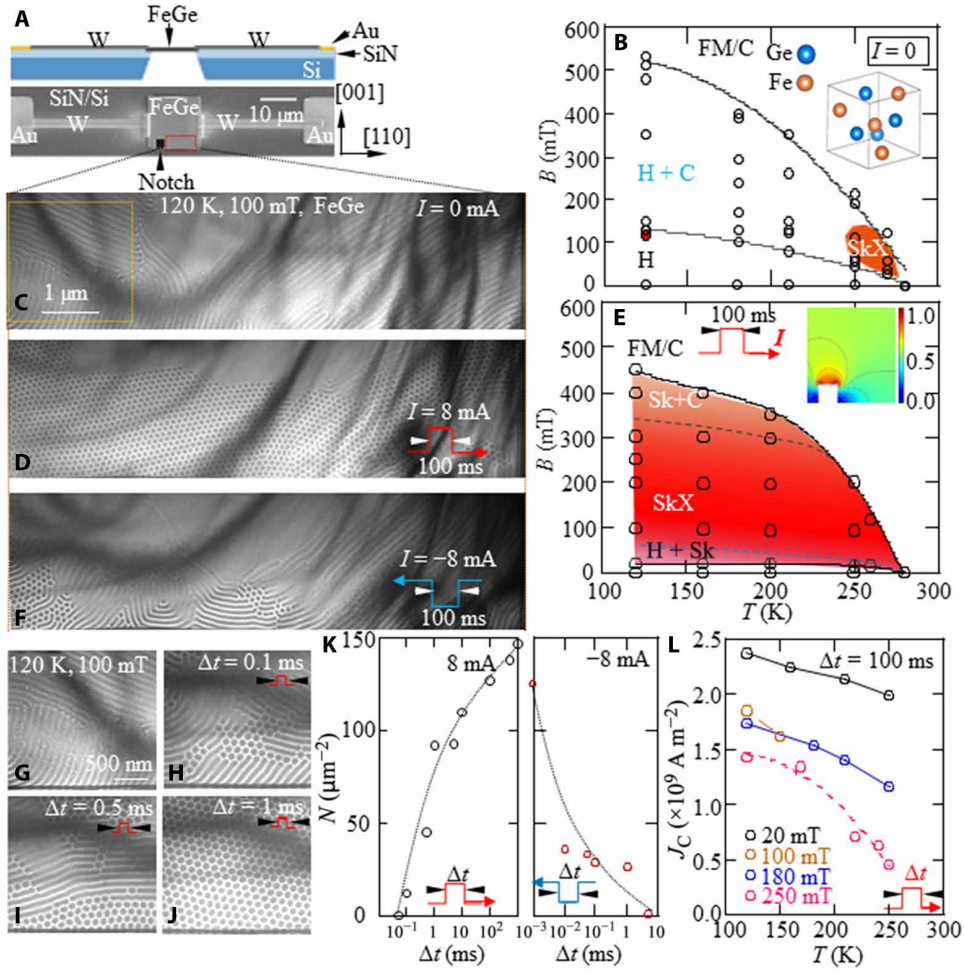

Fig. 1. Creation and extinction of the metastable SkX with unidirectional current injections in a FeGe-based device with a square notch hole. (**A**) Cross-sectional (top; schematic) and top (bottom; a scanning electron microscopy image) views of the device composed of a (110) thin FeGe with electrodes fixed on a SiN/Si-membrane. (**B**) Phase diagram observed in the FeGe without pulsed current flows at various temperature (*T*)–magnetic field (*B*) conditions as specified by open circles. (**C**) Over-focus Lorentz TEM images of helical structure at the current $I = 0$ observed at the area indicated by a red rectangle in (A) at 120 K under a 100-mT normal field. (**D**) Over-focus Lorentz TEM images of metastable SkX generated after one-pulse flow in the plus direction observed at the area indicated by a red rectangle in (A) at 120 K under a 100-mT normal field. (**E**) Phase diagram observed in the FeGe with one pulsed current flows in the plus direction (indicated by the red arrow in the insets) at various temperature (*T*)–magnetic field (*B*) conditions as specified by open circles. (**F**) Helical stripes coexistent with sparsely populated skyrmions after the same pulse as in (D), but flowing in the minus direction. (**G**)Magnified over-focus Lorentz TEM image of the yellow line squared area in (C). (**H** to **J**) Sequentially captured images observed after one-pulse injections with increasing the pulse width Δt. (**K**) Plots of the number (*N*) of skyrmions versus Δt for plus (left) and minus (right) currents, respectively. (L) Temperature dependence of the critical current (J_C) flowing in the plus direction for the nucleation of SkX under several fields. Sk, H, C, and FM denote skyrmion, helical, conical, and the field-aligned FM domain, respectively. Curved lines in phase diagrams show the eye guide for the boundaries among different phases. The inset in (E) shows a simulated contour map of the current density around the notch of the FeGe plate when the current flows in the plus direction. The vertical scale bar indicates the local current density in arbitrary units.

direction at lower temperatures, such as at 120 K. Such SkX is topologically stable, whereas it can be turned into helices by application of the same pulse current but in the "minus" direction (Fig. 1F). The generation/extinction of the metastable SkX with one current pulse flow in the plus/minus direction has also been observed at a conical structure (120 K, 120 mT) (see fig. S2 and movie S1 for details). Systematic Lorentz TEM observations with current pulse flows in the plus direction at various *T* and *B* conditions have directly confirmed the enlargement of SkX phase (Fig. 1E), whereas current flows in the minus direction erase SkX. Figure 1 (G to J) shows a series of Lorentz TEM images observed before (Fig. 1G) and after one-pulse stimulations (Fig.1, H to J) in the plus direction with slightly increasing the pulse width Δt; Δt is limited below 1 ms to suppress the Joule heating in the present FeGe device (*30*). The sequential observations have also been performed with pulse stimulations in the minus direction. Systematically imaging the metastable skyrmions has shown the increase of the number (*N*) of metastable skyrmions as the currents flow with increasing Δt in the plus direction (Fig. 1K, left) and the decrease of *N* as the currents flow in the minus direction (Fig. 1K, right). Figure 1L shows the *T* dependence of J_C for the nucleation of the metastable SkX in the present notched device: J_C decreases with an increase in *B* and/or *T*. All in all, the real-space observations reveal a nonadiabatic unidirectional current effect on generation and extinction of the metastable SkX in the notched device, which is designed to realize local spin current injections induced by inhomogeneous current around the notch (see the

simulated contour map of the current density distribution in the device in the inset of Fig. 1E and fig. S3). The evolution of SkX phase with current flows has also been observed in another device with a notch at the center of the device side (fig. S4E), whereas the phenomenon of generation of SkX is absent in the device without a notch (fig. S4D). Thus, the distinction between "+" and "−" current injections arises from the upper or lower side of the plate, on which the notch is fabricated.

Lorentz TEM observations (Fig. 2) have been performed with finely intensifying pulsed current excitation to trace the current-induced metastable SkX from the thermodynamic nontopological state (helical/conical) in the notched device. At the initial state (120 K, 0 mT), the periodic stripes in a Lorentz TEM image (Fig. 2A), representing the in-plane helices, appear to be almost perpendicular to the upper side of the notch. A short current pulse (I = 10 mA, Δt = 0.1 ms) effectively rotates the stripes (Fig. 2A) to be parallel to the current flow direction (Fig. 2B) except for that at the corner of the notch, which is bent to run along the corner and thereby producing spherical wave–like helices. The rearrangement of helices upon a current stimulation is possibly caused by the coupling among the helical wave vector and the spin-polarized current. By increasing the I and Δt up to 13 mA (current density; 3.3×10^9A m^{-2}) and 10 ms, respectively, a metastable SkX accompanied by short intervening in-plane helices (Fig. 2C; the real-space image and related Fourier transforms) emerges at zero magnetic field. With a further increase of the number of current pulses, the in-plane helices are almost removed, followed by the formation of a nearly perfect SkX in the notched plate of FeGe (see movie S2). When the normal magnetic field of 160 mT is applied at 120 K, the conical structure with the wave vector normal to the thin plate (parallel to the incoming electron beam) is anticipated, although the Lorentz TEM cannot visualize it (Fig. 2D), while short in-plane helices are discerned near the upper edge of the notch. With the fine-tuning of I, Lorentz TEM observations starting from such a conical state have also shown that skyrmions begin to appear around the corners of the notch when the current exceeds a J_C (Fig. 2E); with a further increase in the current injection, they expand over the thin plate, completely transforming the nontopological state into the SkX (Fig. 2, E to G). These Lorentz TEM observations indicate that the local spin current injection arising from the inhomogeneous current (fig. S4C) around the corners of the notch is the key to excite skyrmions. To sum up, such localized spin current injection first induces the rearrangement of helices and then the nucleus of skyrmions (near the corner of the notch, as shown in Fig. 2B), which are followed by the domino-like skyrmion proliferation with the increase in pulse height I and/or width Δt (Fig. 1, H to J, and also see movie S3).

To understand the mechanism of extinction of metastable SkX with the current flows in the minus direction, the following should be taken into account: At lower temperatures, the nontopological state, such as helical/conical phase, is thermodynamically stable (see Fig. 1B); therefore, the metastable SkX as produced by pulsed current may be irreversibly destroyed by external stimuli (*19*). A numerical simulation of a skyrmion creation and extinction has been reported (*7*, *12*). In particular, the crucial role of the notch as the source of the singular magnetic moment configuration for the creation of a skyrmion and its dependence on the current direction were known by the simulations (*7*). However, the background configuration of magnetic moments is assumed to be the FM one in these studies and not the helical/conical phases as in the present study. The current-induced alignment of the helix and also the proliferation of the skyrmions to form the SkX are the experimental findings that are not expected from the earlier theoretical studies. Incidentally, the observed unidirectional current effect provides a compelling evidence for the intrinsic origin of the local spin current injection for the creation of 80-nm skyrmions and the extinction of the metastable SkX, verifying the minor Joule heating effect in the present device.

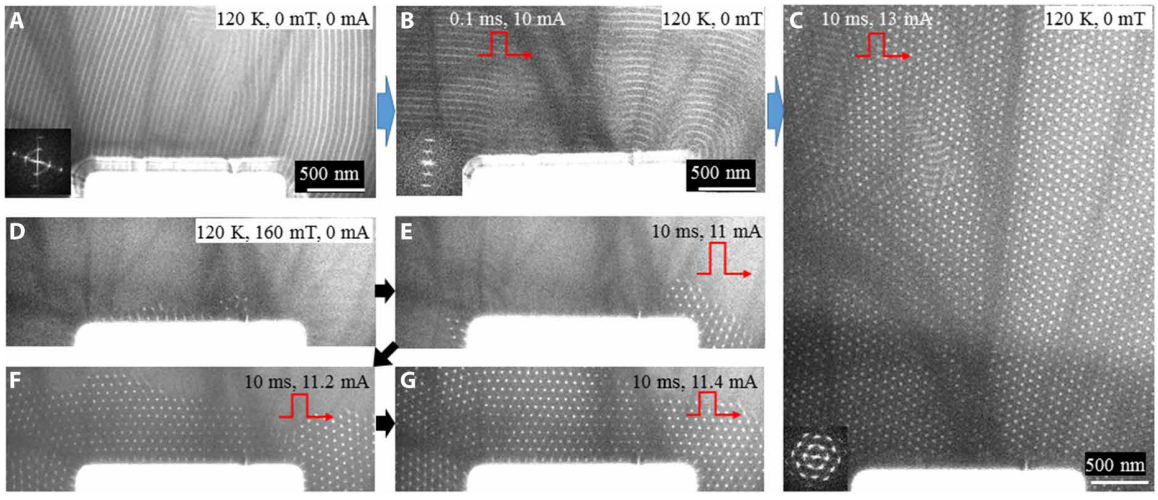

Fig. 2. Formation of a metastable SkX and the rearrangement of helices with electric current injections in a FeGe-based device with a notch. (**A** to **C**) Under-focus Lorentz TEM images showing a helical structure composed of multidomains with a single wave vector (***q***) for the initial state (A; 120 K, 0 mT), helices with ***q*** approximately perpendicular to the current flow direction (indicated by the red arrow) observed after one current pulse injection (B; 10 mA, 0.1 ms), and metastable SkX accompanied by in-plane short helices observed after one pulse excitation with larger I and longer Δt (C; 13 mA, 10 ms), respectively. Insets are Fourier transforms of the corresponding Lorentz TEM images, respectively. (**D** to **G**) Under-focus Lorentz TEM images representing a conical structure accompanied by several skyrmions and short helices near the upper edge of the notch observed at 120 K under 160 mT (D), nucleation of skyrmions near the corners of the notch after one plus current pulse excitation (E; 11 mA, 10 ms), and SkX generated with finely increasing the pulse height I (F and G; 11.2 mA, 11.4 mA). Blue and dark arrows among the panels show the chorological order of Lorentz TEM observations under 0- and 160-mT fields, respectively.

Let us proceed to the current-induced motion of a single 80-nm skyrmion and a few-skyrmion aggregate upon a current pulse stimulation in the notched device; here, we take the current density of 2.4×10^8 A m^{-2} corresponding to the pulse height I of 1.0 mA. First, a single skyrmion (Fig. 3A) was successfully generated: Starting from the metastable SkX, the current pulses flowing in the minus direction were applied while optimizing I and Δt; SkX was progressively destroyed/erased until one single skyrmion was left in the TEM view area. Then, the single skyrmion was driven by current pulses with Δt less than 0.5 ms to avoid any further nucleation or annihilation of skyrmions. A series of Lorentz TEM images upon current pulses can track the skyrmion motion; the skyrmion is deflected by spin-polarized current and moves sequentially from the upper right corner to the lower left corner in the thin plate as I along the plus direction is increased progressively. In contrast, the skyrmion moves in the opposite direction, i.e., from the lower left side to the upper right side of the plate, when the current pulses flow in the minus direction, as shown in Fig. 3 (F to J). These results provide a direct evidence for the translational and Hall motion of the single 80-nm skyrmion, although fluctuations of the skyrmion motion (see Fig. 3, K and L) appear with such small currents close to J_C, which is caused, perhaps, by the random pinning sites in the device.

An interesting torque motion is observed on a skyrmion aggregate with current pulse stimulations. We use short (Δt = 0.1 ms) pulses for drives of the skyrmion aggregate. Figure 4 (A and F) represents initial states of coexistent four-skyrmion aggregate and single skyrmion prepared at 180 K under 175 mT (Fig. 4A) and a three-skyrmion aggregate at 170 K under 200 mT (Fig. 4F) from the originally current-induced metastable skyrmions following the similar procedure as described above. Figure 4 (B to E) shows several Lorentz TEM images observed after pulse stimulations in the plus direction while keeping I at 4 mA and Δt = 0.1 ms, but increasing the number of pulses, while Fig. 4 (G to H) represents the images with current flow in the minus direction with increasing I. As revealed by such sequential Lorentz TEM images, a single skyrmion moves more rapidly than the four-skyrmion aggregate, possibly owing to the different energy barrier and/or trapping events that need to be overcome for movement. Incidentally, in addition to the translational and Hall motions, the skyrmion aggregate exhibits also the internal rotational motion (see Fig. 4, F to H, and movie S4), which directly points to the torque force working on skyrmion aggregate; perhaps this is due to the inhomogeneous local current density and/or pinning sites present around the skrymion aggregate.

The Hall motions of a skyrmion aggregate have been examined also with DC current flows in both plus and minus directions, as shown in Fig. 4 (I to N) (see also movie S5). At the initial states, a chain-like three-skyrmion aggregate settles on the right/left side of the notched device (Fig. 4, I and L). Then, the in situ Lorentz TEM

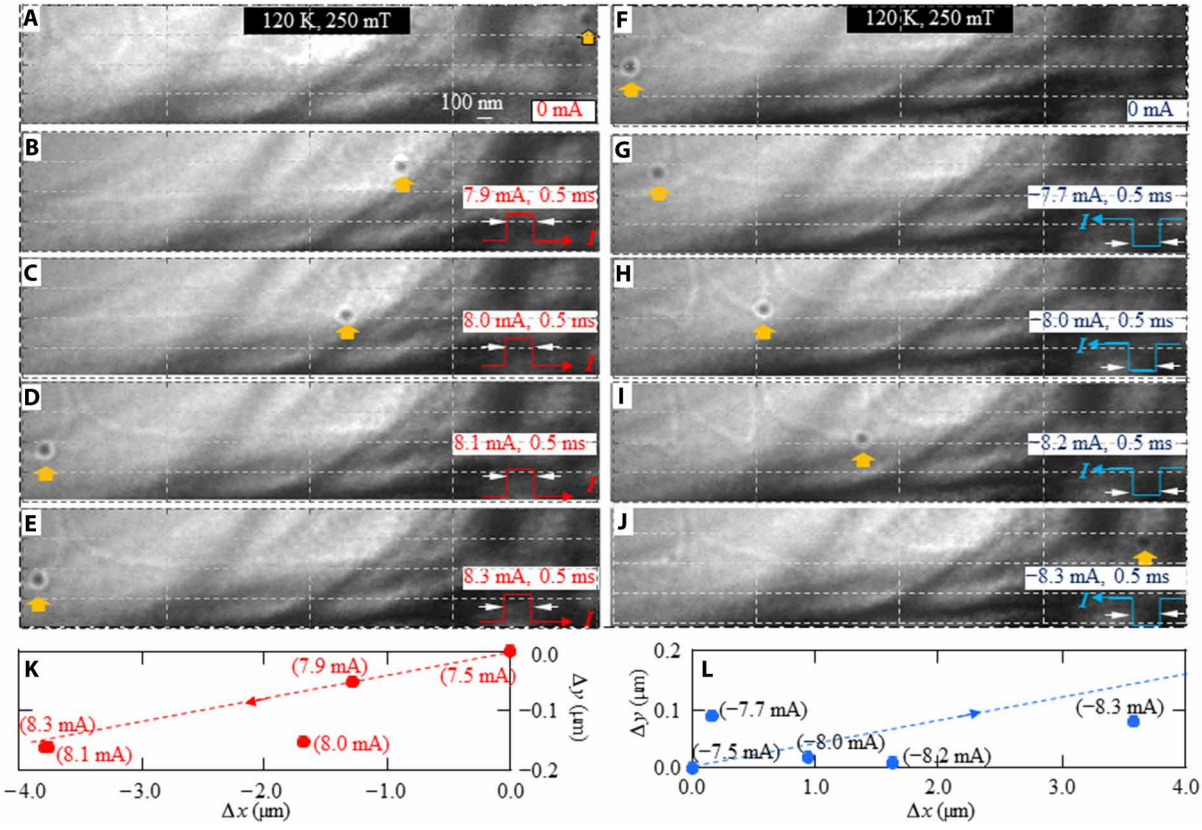

Fig. 3. Direct observations of Hall motion of a single 80-nm skyrmion with current pulse stimulations. (**A** to **J**) Over-focus Lorentz TEM images observed after current stimulations at 120 K under a 250-mT field with varying I for each current direction, while keeping Δt constant (=0.5 ms). The cells in (A) to (J) are eye guides for scale (1 and 0.1 μm). (**K** and **L**) Plot of displacements of the skyrmion along (Δx) and vertical to (Δy) the electron flow direction with various current stimulations, respectively, measured from the original position, $\Delta x = \Delta y = 0$. Closed circles and dashed lines with arrows show the experimental data points and the linear fittings of $\frac{\Delta y}{\Delta x}$ for the averaged Hall angle, respectively.

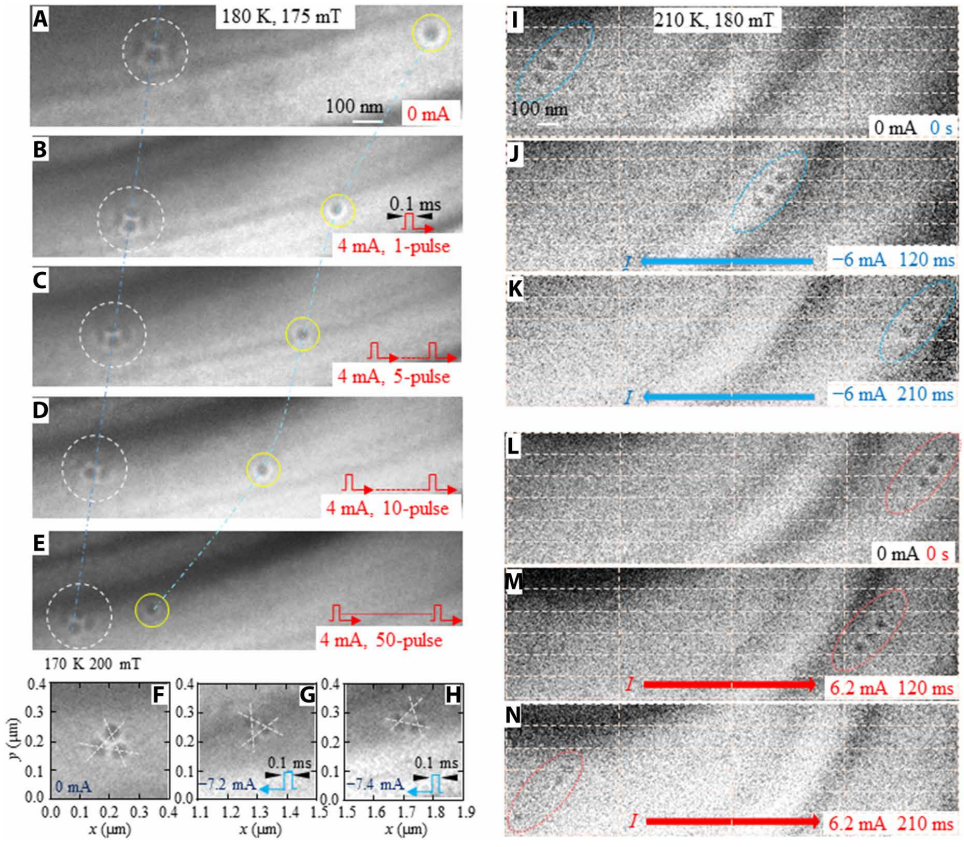

Fig. 4. Torque and Hall motions of few-skyrmion aggregates with current stimulations. (**A** to **H**) Motions stimulated by pulsed currents. (**I** to **N**) Motions stimulated by DC currents. (A and F, I and L) States without current injection. (B to E) Keeping the current strength and pulse width while increasing the number of pulse. (G to H) One current pulse injections with a increase of current strength. (J to K) DC currents flows in minus direction. (M to N) DC currents flow in plus direction.

movies capture its motions with DC current flows in each direction. The displacements of the skyrmion aggregate are clearly revealed by a series of Lorentz TEM snapshots at several elapsed time points (Fig. 4, I to K and L to N) with current flows in the plus/minus direction. This indicates that the skyrmion aggregate moves along the electron flows with a Hall angle of about 9° in the present case. This Hall angle is rather large, which is probably enhanced near J_C due to the pinning force by impurities (*31*). The Hall motions of the skyrmion aggregate at 210 K with DC current flow confirms again that the spin transfer torque effect governs skyrmion-aggregate dynamics as well.

DISCUSSION

We have demonstrated the creation and extinction of 80-nm skyrmions in a FeGe-based device with directional current pulses. Current-induced drift, Hall, and torque motions of the single skyrmions and their aggregates can be tracked by using low current densities (0.96×10^9 to 1.92×10^9 A m^{-2}), which are three orders of magnitude smaller than those for drives of magnetic domain walls in typical racetrack memory (*1*). On the other hand, from the viewpoint of skyrmion-based devices, the skyrmion Hall motion in the present device should limit the moving distance. To solve this problem, the antiferromagnetically exchange-coupled bilayer system hosting combined skyrmions (*32*) would be promising and applicable also to the chiral magnets like the present case with an appropriate choice of spacer material (*33*).

MATERIALS AND METHODS

Preparation of a notched device

The notched device was prepared as follows: (i) The thin plate (14.2 μm by 14.2 μm by 0.3 μm) of (110) FeGe (fig. S1A; SEM image) with a notch hole (2.5 μm by 2.5 μm) was prepared by thinning a bulk FeGe using a microsampling technique with a focused-ion-beam system (NB-5000, Hitachi); (ii) a Si membrane was prepared with coating 50-nm SiN and four electrodes (Au) (fig. S1B; SEM image) were fabricated by e-beam lithography; (iii) a thin tungsten (W) film was deposited on the two sides of the FeGe thin plate placed on the membrane; and (iv) the thin plate and electrodes were connected by W wires (fig. S1C; SEM image). The geometry and thickness of the FeGe plate were characterized in terms of SEM images.

Lorentz TEM observations of skyrmions with current flows

All the real-space observations of skyrmions in the devices were performed at the Lorentz TEM mode after zero-field cooling. In the defocused Lorentz TEM images, skyrmions with clockwise/counterclockwise helicity can be viewed as bright/dark dots owing to the interaction between the incident electrons and the in-plane magnetizations in skyrmions [see (*17*)].

The devices were settled on the TEM sample stage within the objective lens (coil), therefore accepting a normal field induced by the lens (coil) current. The residual field was approximately 7 mT when the objective lens current was switched off, which was measured by a Hall probe mounted on the sample stage. All the images

were recorded by a fast-imaging camera (Gatan, OneView) attached to a multifunctional TEM (JEM-2800).

SUPPLEMENTARY MATERIALS

Supplementary material for this article is available at http://advances.sciencemag.org/cgi/content/full/6/25/eaaz9744/DC1

REFERENCES AND NOTES

1. S. S. P. Parkin, M. Hayashi, L. Thomas, Magnetic domain-wall racetrack memory. *Science* **320**, 190–194 (2008).
2. F. Jonietz, S. Mühlbauer, C. Pfleiderer, A. Neubauer, W. Münzer, A. Bauer, T. Adams, R. Georgii, P. Boni, R. A. Duine, K. Everschor, M. Garst, A. Rosch, Spin transfer torques in MnSi at ultralow current densities. *Science* **330**, 1648–1651 (2010).
3. X. Z. Yu, N. Kanazawa, W. Z. Zhang, T. Nagai, T. Hara, K. Kimoto, Y. Matsui, Y. Onose, Y. Tokura, Skyrmion flow near room temperature in an ultralow current density. *Nat. Commun.* **3**, 988 (2012).
4. T. Schulz, R. Ritz, A. Bauer, M. Halder, M. Wagner, C. Franz, C. Pfleiderer, K. Everschor, M. Garst, A. Rosch, Emergent electrodynamics of skyrmions in a chiral magnet. *Nat. Phys.* **8**, 301–304 (2012).
5. T. Kurumaji, T. Nakajima, M. Hirschberger, A. Kikkawa, Y. Yamasaki, H. Sagayama, H. Nakao, Y. Taguchi, T.-h. Arima, Y. Tokura, Skyrmion lattice with a giant topological Hall effect in a frustrated triangular-lattice magnet. *Science* **365**, 914–918 (2019).
6. N. Nagaosa, Y. Tokura, Topological properties and dynamics of magnetic skyrmions. *Nat. Nanotechnol.* **8**, 899–911 (2013).
7. J. Iwasaki, M. Mochizuki, N. Nagaosa, Current-induced skyrmion dynamics in constricted geometries. *Nat. Nanotechnol.* **8**, 742–747 (2013).
8. J. Iwasaki, W. Koshibae, N. Nagaosa, Colossal spin transfer torque effect on skyrmion along the edge. *Nano Lett.* **14**, 4432–4437 (2014).
9. H. Oike, A. Kikkawa, N. Kanazawa, Y. Taguchi, M. Kawasaki, Y. Tokura, F. Kagawa, Interplay between topological and thermodynamic stability in a metastable magnetic skyrmion lattice. *Nat. Phys.* **12**, 62–66 (2016).
10. S. Woo, K. Litzius, B. Krüger, M.-Y. Im, L. Caretta, K. Richter, M. Mann, A. Krone, R. M. Reeve, M. Weigand, P. Agrawal, I. Lemesh, M. A. Mawass, P. Fischer, M. Kläui, G. S. D. Beach, Observation of room-temperature magnetic skyrmions and their current-driven dynamics in ultrathin metallic ferromagnets. *Nat. Mater.* **15**, 501–506 (2016).
11. W. Jiang, P. Upadhyaya, W. Zhang, G. Yu, M. B. Jungfleisch, F. Y. Fradin, J. E. Pearson, Y. Tserkovnyak, K. L. Wang, O. Heinonen, S. G. E. te Velthuis, A. Hoffmann, Blowing magnetic skyrmion bubbles. *Science* **349**, 283–286 (2015).
12. J. Sampaio, V. Cros, S. Rohart, A. Thiaville, A. Fert, Nucleation, stability and current-induced motion of isolated magnetic skyrmions in nanostructures. *Nat. Nanotechnol.* **8**, 839–844 (2013).
13. W. Jiang, X. Zhang, G. Yu, W. Zhang, X. Wang, M. Benjamin Jungfleisch, J. E. Pearson, X. Cheng, O. Heinonen, K. L. Wang, Y. Zhou, A. Hoffmann, S. G. E. te Velthuis, Direct observation of the skyrmion Hall effect. *Nat. Phys.* **13**, 162–169 (2017).
14. A. Hrabec, J. Sampaio, M. Belmeguenai, I. Gross, R. Weil, S. M. Chérif, A. Stashkevich, V. Jacques, A. Thiaville, S. Rohart, Current-induced skyrmion generation and dynamics in symmetric bilayers. *Nat. Commun.* **8**, 15765 (2017).
15. L. Caretta, M. Mann, F. Büttner, K. Ueda, B. Pfau, C. M. Günther, P. Hessing, A. Churikova, C. Klose, M. Schneider, D. Engel, C. Marcus, D. Bono, K. Bagschik, S. Eisebitt, G. S. D. Beach, Fast current-driven domain walls and small skyrmions in a compensated ferrimagnet. *Nat. Nanotechnol.* **13**, 1154–1160 (2018).
16. K. Karube, J. S. White, N. Reynolds, J. L. Gavilano, H. Oike, A. Kikkawa, F. Kagawa, Y. Tokunaga, H. M. Rønnow, Y. Tokura, Y. Taguchi, Robust metastable skyrmions and their triangular–square lattice structural transition in a high-temperature chiral magnet. *Nat. Mater.* **15**, 1237–1242 (2016).
17. X. Z. Yu, D. Morikawa, T. Yokouchi, K. Shibata, N. Kanazawa, F. Kagawa, T.-h. Arima, Y. Tokura, Aggregation and collapse dynamics of skyrmions in a non-equilibrium state. *Nat. Phys.* **14**, 832–836 (2018).
18. L. Desplat, D. Suess, J.-V. Kim, R. L. Stamps, Thermal stability of metastable magnetic skyrmions: Entropic narrowing and significance of internal eigenmodes. *Phys. Rev. B* **98**, 134407 (2018).
19. F. Kagawa, H. Oike, W. Koshibae, A. Kikkawa, Y. Okamura, Y. Taguchi, N. Nagaosa, Y. Tokura, Current-induced viscoelastic topological unwinding of metastable skyrmion strings. *Nat. Commun.* **8**, 1332 (2017).
20. X. Z. Yu, D. Morikawa, Y. Tokunaga, M. Kubota, T. Kurumaji, H. Oike, M. Nakamura, F. Kagawa, Y. Taguchi, T.-h. Arima, M. Kawasaki, Y. Tokura, Current-induced nucleation and annihilation of magnetic skyrmions at room temperature in a chiral magnet. *Adv. Mater.* **29**, 1606178 (2017).
21. K. Shibata, T. Tanigaki, T. Akashi, H. Shinada, K. Harada, K. Niitsu, D. Shindo, N. Kanazawa, Y. Tokura, T. H. Arima, Current-driven motion of domain boundaries between skyrmion lattice and helical magnetic structure. *Nano Lett.* **18**, 929–933 (2018).
22. T. Yokouchi, S. Hoshino, N. Kanazawa, A. Kikkawa, D. Morikawa, K. Shibata, T.-h. Arima, Y. Taguchi, F. Kagawa, N. Nagaosa, Y. Tokura, Current-induced dynamics of skyrmion strings. *Sci. Adv.* **4**, eaat1115 (2018).
23. W. Legrand, D. Maccariello, N. Reyren, K. Garcia, C. Moutafis, C. Moreau-Luchaire, S. Collin, K. Bouzehouane, V. Cros, A. Fert, Room-temperature current-induced generation and motion of sub-100 nm skyrmions. *Nano Lett.* **17**, 2703–2712 (2017).
24. F. Büttner, I. Lemesh, M. Schneider, B. Pfau, C. M. Günther, P. Hessing, J. Geilhufe, L. Caretta, D. Engel, B. Krüger, J. Viefhaus, S. Eisebitt, G. S. D. Beach, Field-free deterministic ultrafast creation of magnetic skyrmions by spin–orbit torques. *Nat. Nanotechnol.* **12**, 1040–1044 (2017).
25. Y. Yamane, J. Sinova, Skyrmion-number dependence of spin-transfer torque on magnetic bubbles. *J. Appl. Phys.* **120**, 233901 (2016).
26. K. Everschor-Sitte, J. Masell, R. M. Reeve, M. Klaüi, Perspective: Magnetic skyrmions—Overview of recent progress in an active research field. *J. Appl. Phys.* **124**, 240901 (2018).
27. X. Z. Yu, N. Kanazawa, Y. Onose, K. Kimoto, W. Z. Zhang, S. Ishiwata, Y. Matsui, Y. Tokura, Near room-temperature formation of a skyrmion crystal in thin-films of the helimagnet FeGe. *Nat. Mater.* **10**, 106–109 (2011).
28. J. C. Loudon, A. O. Leonov, A. N. Bogdanov, M. Ciomaga Hatnean, G. Balakrishnan, Direct observation of attractive skyrmions and skyrmion clusters in the cubic helimagnet Cu_2OSeO_3. *Phys. Rev. B* **97**, 134403 (2018).
29. A. O. Leonov, Y. Togawa, T. L. Monchesky, A. N. Bogdanov, J. Kishine, Y. Kousaka, M. Miyagawa, T. Koyama, J. Akimitsu, T. Koyama, K. Harada, S. Mori, D. McGrouther, R. Lamb, M. Krajnak, S. McVitie, R. L. Stamps, K. Inoue, Chiral surface twists and skyrmion stability in nanolayers of cubic helimagnets. *Phys. Rev. Lett.* **117**, 087202 (2016).
30. X. Zhao, S. Wang, C. Wang, R. Che, Thermal effects on current-related skyrmion formation in a nanobelt. *Appl. Phys. Lett.* **112**, 212403 (2018).
31. J. Iwasaki, M. Mochizuki, N. Nagaosa, Universal current–velocity relation of skyrmion motion in chiral magnets. *Nat. Commun.* **4**, 1463 (2013).
32. X. Zhang, Y. Zhou, M. Ezawa, Magnetic bilayer-skyrmions without skyrmion Hall effect. *Nat. Commun.* **7**, 10293 (2016).
33. W. Legrand, D. Maccariello, F. Ajejas, S. Collin, A. Vecchiola, K. Bouzehouane, N. Reyren, V. Cros, A. Fert, Room-temperature stabilization of antiferromagnetic skyrmions in synthetic antiferromagnets. *Nat. Mater.* **19**, 34–42 (2020).

Acknowledgments: We thank S. Maekawa, W. Koshibae, T. Kagawa, H. Oike, and Y. Taguchi for discussions. **Funding:** This work was supported in part by Grants-In-Aid for Scientific Research (A) (grant no. 19H0066014 and 18H03676) from the Japan Society for the Promotion of Science (JSPS) and the Japan Science and Technology Agency (JST) CREST program (grant number JPMJCR1874), Japan. **Author contributions:** X.Z.Y. and Y.T. conceived the project and wrote the manuscript. X.Z.Y. performed Lorentz TEM observations and analyzed the experimental data with N.N. and Y.T. X.Z.Y., D.M., and K.N. designed and fabricated the microdevice. K.S. and T.A. simulated the current density in the device. N. K. synthesized the bulky FeGe. All authors discussed the data and commented on the manuscript. **Competing interests:** The authors declare that they have no competing interests. **Data and materials availability:** All data needed to evaluate the conclusions in the paper are present in the paper and/or the Supplementary Materials. Additional data related to this paper may be requested from the authors.

Submitted 24 October 2019
Accepted 5 May 2020
Published 17 June 2020
10.1126/sciadv.aaz9744

Citation: X. Z. Yu, D. Morikawa, K. Nakajima, K. Shibata, N. Kanazawa, T. Arima, N. Nagaosa, Y. Tokura, Motion tracking of 80-nm-size skyrmions upon directional current injections. *Sci. Adv.* **6**, eaaz9744 (2020).

Motion tracking of 80-nm-size skyrmions upon directional current injections

X. Z. Yu, D. Morikawa, K. Nakajima, K. Shibata, N. Kanazawa, T. Arima, N. Nagaosa and Y. Tokura

Sci Adv **6** (25), eaaz9744.
DOI: 10.1126/sciadv.aaz9744